Research on Turning Characteristics of Helicopter Ground Motion

LI Jin[1,2] , *ZHANG Ming*[2*] , *HUANG Jianxin*[1] , *CHEN Xiang*[1] , *WEI Xiyang*[2]

1. China Helicopter Research and Development Institute，Jingdezhen 333001，P. R. China；

2. Key Laboratory of Fundamental Science for National Defense-Advanced Design Technology of Flight Vehicle，
Nanjing University of Aeronautics and Astronautics，Nanjing 210016，P. R. China

Abstract: In the passive turning state，the helicopter turns through the tail rotor force and the friction of the ground to the tire. In practice，it is found that the helicopter will turn difficultly under low aircraft ground speed or static state. This paper takes a certain type of helicopter as the research object，and establishes the dynamic model of helicopter ground turning motion based on the basic theory of dynamics. This model takes into account the six-degree-of-freedom motion model of the helicopter body，the motion model of the landing gear buffer，the tire mechanics model and the friction characteristics of the strut friction disc. The dynamic simulation of the helicopter right angle turn and static turn is carried out，and the influence of parameters such as tail rotor pull，taxi speed，tail wheel stability distance on the dynamic response of the turn is studied. The results show that under the same ground taxing speed，the tail wheel angle increases with the increase of tail rotor force. When the tail rotor force is the same，the tail wheel angle increases with the increase of ground taxing speed. When the helicopter is completely static，it is the most difficult to turn，which requires much bigger force of the tail rotor to turn. In addition，the change of the stability distance of the tail wheel has an obvious influence on the turning. When the stability distance is doubled，the tail rotor force will be reduced by 30％ to the same angle of the tail wheel.

Key words：helicopter ground motion；dynamics analysis；passive turning；landing gear

CLC number：V226　　　　**Document code**：A　　　　**Article ID**：1005-1120（2022）05-0593-13

0　Introduction

When the rear three-point layout of helicopter is turning on the ground，it is mainly turned by differential braking or the tail rotor force[1-4]. This paper mainly studies the situation that the helicopter turns by the tail rotor force at low speed. The force of the tail rotor drives the helicopter and tires to produce lateral motion，which deflects the tail wheel and the axis of rotation，thus realizing the helicopter turning，which belongs to the passive turning mode[5]. In practice，its rocker arm has a large turn friction torque for the shimmy need of the tail wheel[6]. Therefore，the turning process is divided into two steps：（1）When the tail rotor force is small，the tail rotor provides lateral load to drive the tires produce side-slip motion. At this time，the torque generated by the lateral force of the tail wheel cannot overcome the friction torque，and the tail wheel state does not deflect. （2）When the tail rotor force increases to a higher level，the deflection of helicopter will intensify. The torque generated by the lateral force of tail wheel can overcome the friction torque and drive the rocker arm to rotate，the wheel will turn a angle，and the helicopter enters the normal turning state[7-10].

In order to analyze the motion of helicopter under different speeds and tail rotor force，the dynamic equation of helicopter tail wheel passive turning is established in this paper. In the model，many factors

are considered to solve the force and motion characteristics of the helicopter in the whole process of passive turning, such as the overall layout of the helicopter, the structural layout of the tail landing gear, the dynamic characteristics of the tire, the speed of the helicopter, and the tail rotor force.

1 Mathematical Modeling of Helicopter Ground Turning Motion

1. 1 Basic hypothesis of model

In order to make the model accurate and practical, the model should be simplified and assumed appropriately[11] to reduce the uncertainty factors caused by some parameters that are difficult to determine and the accumulation of errors caused by too many degrees of freedom and constraints. And the following assumptions are made for the model[12-13]:

(1) The helicopter is divided into two parts: elastic support mass and inelastic support mass. The elastic support mass includes the helicopter body supported by the buffer, the outer cylinder of the buffer. While the inelastic support mass includes the buffer piston rod, the wheel, the brake device and other auxiliary mechanisms.

(2) The motion of the elastic support mass is six degrees of freedom, and the mass is concentrated at the center of mass of the fuselage. The motion of the inelastic support mass only considers the translational degrees of freedom in three directions, ignoring the lateral deformation and torsional deformation of the buffer.

(3) Each wheel has an independent degree of rotational freedom.

(4) Ignoring the aerodynamic load of the inelastic support mass, the main rotor force and tail rotor force are treated as concentrated forces, which act on the center of gravity of the helicopter and the center of the tail rotor respectively.

According to the geometric characteristics of the helicopter, the ground turning diagram is established, as shown in Fig.1.
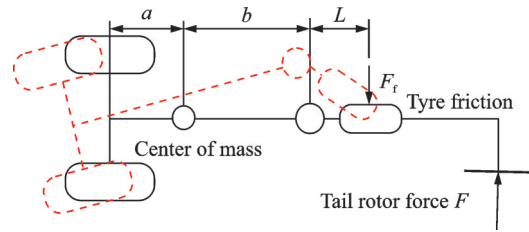
Fig.1   Helicopter ground turning diagram

1. 2 Definition and transformation of coordinate system

When the helicopter is moving on the ground, it is subject to gravity, the rotor pull, the tail rotor lateral force, and the force of ground on the tires. Different forces need to be expressed in different coordinate systems. The definition of the coordinate system is as follows.

As shown in Fig.2, in the ground coordinate system $O_i\text{-}X_iY_iZ_i$, the center of mass of helicopter in the initial state is taken as the coordinate origin, the axis X_i is parallel to the center line of runway and points to the forward direction of the helicopter, the axis Y_i is perpendicular to the axis X_i in the horizontal plane, and the axis Z_i is vertically downward. In Fig.2, θ is the pitch angle, ψ is the roll angle and ϕ is the yaw angle.
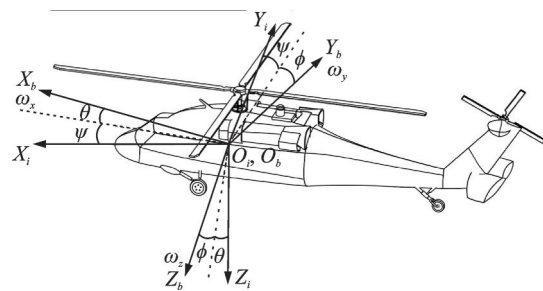
Fig.2   Relationship between ground inertial coordinate system and airframe coordinate system

In the airframe coordinate $O_b\text{-}X_bY_bZ_b$, the center of mass of helicopter is taken as the coordinate origin, fixed with the helicopter, the axis X_b points forward along the axis of the helicopter body, the axis Y_b is perpendicular to the axis X_b in the horizontal plane, and the axis Z_b follows the right-hand rule and goes down vertically.

In the wheel coordinate system $O_j\text{-}X_jY_jZ_j$, the

rotation center of the wheel is taken as the coordinate origin, the axis X_j points to the forward direction of the wheel, the axis Z_j is perpendicular to the axis X_j and vertically downwards, and the axis Y_j points to the right according to the right-hand rule.

1.3 Helicopter dynamics model

When the helicopter is moving on the ground, it is subject to gravity, the rotor force, the tail rotor lateral force, and the force of ground on the tires. The forces that the ground on the tires include longitudinal friction, lateral friction, vertical support reaction force, and righting torque.

The translational equation of the helicopter body center of mass is established in the ground inertial coordinate system, which can be written as

$$m\begin{pmatrix}\ddot{x}\\\ddot{y}\\\ddot{z}\end{pmatrix}=T_{ib}\left(\boldsymbol{P}+\boldsymbol{G}+\sum_i T_{bj}\begin{bmatrix}F_{xi}\\F_{yi}\\F_{zi}\end{bmatrix}+\boldsymbol{T}\right)\quad(1)$$

where T_{ib} is the transformation matrix from the body coordinate system to the inertial coordinate system; T_{bj} the transformation matrix from the wheel coordinate system to the body coordinate system, in which j is the j landing gear; G the gravity matrix in the body coordinate system; T the tail rotor force matrix in the body coordinate system; m the body mass; $[\ddot{x}\quad\ddot{y}\quad\ddot{z}]^T$ the acceleration vector of the body mass center; P the force matrix of rotor tension acting on the body; and $[F_{xj}\quad F_{yj}\quad F_{zj}]^T$ the force of each landing gear on the body.

The equation of helicopter body rotation around the center of mass can be written as

$$\boldsymbol{I\dot{\omega}}+\boldsymbol{\omega I\omega}=\sum_i\left(\begin{bmatrix}M_{xi}\\M_{yi}\\M_{zi}\end{bmatrix}-R_{bj}\begin{bmatrix}F_{xi}\\F_{yi}\\F_{zi}\end{bmatrix}\right)+\boldsymbol{M}_P+\boldsymbol{M}_T\quad(2)$$

$$\boldsymbol{I}=\begin{bmatrix}I_{xx}&-I_{xy}&-I_{xz}\\-I_{yx}&I_{yy}&-I_{yz}\\-I_{zx}&-I_{zy}&I_{zz}\end{bmatrix}\quad(3)$$

$$\boldsymbol{\omega}=\begin{bmatrix}0&-\omega_z&\omega_y\\\omega_z&0&-\omega_x\\-\omega_y&\omega_x&0\end{bmatrix}\quad(4)$$

$$\boldsymbol{R}_{bi}=\begin{bmatrix}0&-R_{zi}&R_{yi}\\R_{zi}&0&-R_{xi}\\-R_{yi}&R_{xi}&0\end{bmatrix}\quad(5)$$

where I is the matrix of the moment of inertia of the helicopter body; ω the matrix of the angular velocity of the helicopter body rotating around the center of mass; R_{bj} the matrix of the distance between the connection point of each landing gear and the airframe to the center of mass; $[M_{xj}\ M_{yj}\ M_{zj}]$ the action torque of each landing gear on the body; M_P the moment matrix of rotor tension acting on the body; M_T the tail rotor moment matrix in the body coordinate system.

Angular velocity $\boldsymbol{\omega}=(\omega_x,\omega_y,\omega_z)^T$, the relationship between the angular velocity component and the derivative of the attitude angle is given by

$$\begin{cases}\dot{\psi}=(\omega_z\cos\phi+\omega_y\sin\phi)/\cos\theta\\\dot{\theta}=\omega_y\cos\phi-\omega_z\sin\phi\\\dot{\phi}=\omega_x+\tan\theta(\omega_z\cos\phi+\omega_y\sin\phi)\end{cases}\quad(6)$$

where $\dot{\psi}$ is the pitch angular velocity; $\dot{\theta}$ the yaw angular velocity; and $\dot{\phi}$ the roll angular velocity.

The force analysis of the inelastic support mass including the piston rod of the landing gear buffer and the wheel is carried out. According to Newton's second law, the dynamic equation of the inelastic support mass is listed as

$$M_{gj}\begin{Bmatrix}\ddot{x}_{gj}\\\ddot{y}_{gj}\\\ddot{z}_{gj}\end{Bmatrix}=T_{ji}^T\begin{Bmatrix}F_{xj}\\F_{yj}\\F_{zj}\end{Bmatrix}+\begin{Bmatrix}0\\0\\W_{gj}\end{Bmatrix}+\begin{Bmatrix}\tilde{F}_{xj}\\\tilde{F}_{yj}\\\tilde{F}_{zj}\end{Bmatrix}\quad(7)$$

where M_{gj} is the inelastic support mass of a single landing gear; $[\ddot{x}_{gj},\ddot{y}_{gj},\ddot{z}_{gj}]^T$ the acceleration vector of the inelastic support mass; T_{ji} the transformation matrix from the ground coordinate system to the wheel coordinate system; $[F_{xjk},F_{yjk},F_{zjk}]^T$ the tire force of each wheel; W_{gi} the gravity of the inelastic support mass; and $[\tilde{F}_{xj},\tilde{F}_{yj},\tilde{F}_{zj}]^T$ the reaction force exerted by the helicopter body on the landing gear.

1.4 Mathematical model of related forces

1.4.1 Mechanical model of landing gear buffer

The paper chooses single chamber oil pneumatic shock absorber as the landing gear buffer. The buffer strut force f_s is composed of air spring force f_a, oil damping force f_d and structural restriction force. Then the total buffer strut force can be written by [14-15]

$$f_s = \begin{cases} K_S S & S < S_0 \\ f_a + f_d & S_0 \leqslant S < S_{max} \\ K_S(S - S_{max}) & S \geqslant S_{max} \end{cases} \tag{8}$$

where K_S is the limited stiffness of the force and compression structures of the buffer related to the structural restriction force; S the buffer stroke; S_0 the stroke when the buffer is fully extended; and S_{max} the stroke when the buffer reaches its maximum compression.

The air spring force f_a is related to the inflation volume, inflation pressure, and buffer compression, and has a non-linear positive correlation with the buffer compression. It can be expressed as

$$f_a = A_a \left[P_0 \left(\frac{V_0}{V_0 - A_a S} \right)^n - P_{atm} \right] \tag{9}$$

where A_a is the air pressure area of the piston; P_0 the initial inflation pressure of the buffer; V_0 the initial inflation volume of the buffer; P_{atm} the local atmospheric pressure; and n the polytropic index of air, generally ranging from 1.0 to 1.3.

The oil damping force f_d is related to the compression speed of the buffer, the area of the oil hole and the effective oil pressure area of the buffer. The direction of the oil damping force is opposite in the positive stroke and the reverse stroke. The oil damping force f_d is expressed by

$$f_d = \left(\frac{\rho_o A_{oz}^3}{2 C_{dz}^2 A_{hz}^2} + \frac{\rho_o A_{oc}^3}{2 C_{dc}^2 A_{hc}^2} \right) \dot{s} |\dot{s}| \tag{10}$$

where ρ_o is the filling oil density of the buffer; A_{oz} and A_{oc} are the effective oil pressure areas of the main oil cavity and the side oil cavity of the buffer, respectively; C_{dz} and C_{dc} the oil hole shrinkage coefficients of the main oil cavity and the side oil cavity, respectively; A_{hz} and A_{hc} the areas of the main oil hole and the side oil hole, respectively .

1.4.2   Gravity and rotor force

The gravity of the helicopter acts on the center of mass of the helicopter and does not have torque effect on the helicopter, which is expressed in the ground inertial coordinate system and can be given by

$$G = \begin{bmatrix} 0 \\ 0 \\ mg \end{bmatrix} \tag{11}$$

where g is the acceleration of gravity, $g = 9.81$ m/s^2.

The main rotor force generally acts in the longitudinal symmetry plane of the helicopter, and its line of action generally does not pass through the center of mass, and there is a certain distance e_p from the center of mass. The rotor force is not parallel to the direction of gravity, but has a forward inclination angle η_1, which causes the helicopter to move forward in the ground taxiing process. The rotor force is expressed in the airframe coordinate system as

$$P = \begin{bmatrix} P \sin \eta_1 \\ 0 \\ -P \cos \eta_1 \end{bmatrix} \tag{12}$$

The rotor force torque is expressed in the airframe coordinate system as

$$M_P = \begin{bmatrix} 0 \\ P e_p \cos \eta_1 \\ 0 \end{bmatrix} \tag{13}$$

1.4.3   Mechanical model of tail rotor force

The tail rotor force acts on the tail beam of the helicopter, which is perpendicular to the symmetrical plane of the helicopter body, and has a certain distance e_T from the center of mass, which generates a lateral turning torque for the helicopter. The tail rotor force is not in the longitudinal plane of symmetry of the helicopter. Viewed from the tail of the helicopter, there is an upward angle of 20° with the longitudinal plane of symmetry, taking η_2. The tail rotor force and torque are expressed in the airframe coordinate system as

$$M_T = \begin{bmatrix} 0 \\ -T e_T \sin \eta_2 \\ T e_T \cos \eta_2 \end{bmatrix} \tag{14}$$

$$T = \begin{bmatrix} 0 \\ T \cos \eta_2 \\ T \sin \eta_2 \end{bmatrix} \tag{15}$$

Due to the high-speed rotation of the main rotor, the helicopter produces a reaction torque. In order to balance this torque, in addition to the force T required for turning, the tail rotor also has a force T_1 to balance the reaction torque. The tail rotor force and torque are expressed in the airframe coordinate system as

$$T = \begin{bmatrix} 0 \\ (T + T_1)\cos\eta_2 \\ (T + T_1)\sin\eta_2 \end{bmatrix} \tag{16}$$

$$M_T = \begin{bmatrix} 0 \\ -(T + T_1)e_T\sin\eta_2 \\ (T + T_1)e_T\cos\eta_2 \end{bmatrix} \tag{17}$$

1.4.4   Tire mechanics model

The NASA tr64 tire model is adopted for this tire study. The characteriastics of the tire are considered in this model concluding longitudinal slip, side slip, vertical compression, the vertical support reaction force longitudinal friction and lateral friction[3]. Fig.3 shows the NASA tr64 semi empirical tire model.
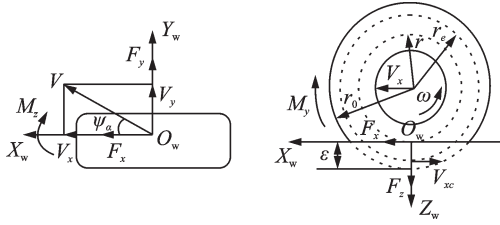
Fig.3   Wheel coordinate system and force diagram

(1) Vertical support reaction force

$$F_z = K_T\delta - C_T\dot{\delta} \tag{18}$$

where K_T is the tire vertical vibration stiffness coefficient, C_T the tire vertical vibration damping coefficient, δ the tire compression, and $\dot{\delta}$ the tire compression speed.

(2) Longitudinal friction

Longitudinal friction is related to the combination coefficient of the tire and the vertical load on the tire, which can be expressed as

$$F_x = \mu_x F_z \tag{19}$$

where μ_x is the longitudinal sliding friction coefficient. Although the relationship between the longitudinal sliding friction coefficient and the longitudinal slip rate is complicated, the coefficient can be given by empirical formula in the calculation of this chapter (Fig.4).

In Fig.4, μ_t is the heading friction coefficient of the tire, and the slip rate is expressed as

$$S_t = (V_x - \omega R_e)/V_x \tag{20}$$

where V_x is the longitudinal velocity of the wheel, ω the rotational angular velocity of the wheel, R_e the rotational radius of the wheel and can be ex-
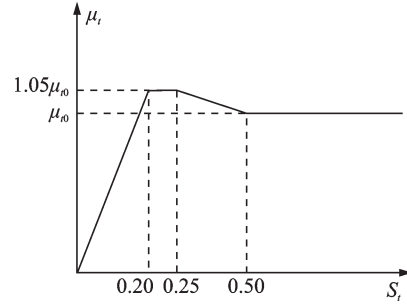
Fig.4   Relationship between slip ratio and longitudinal friction coefficient of tire

pressed as

$$R_e = R_0 - \frac{1}{3}\delta \tag{21}$$

(3) Lateral friction

The lateral friction of the tire is related to the lateral and longitudinal velocity of the tire, the coefficient of lateral friction and the vertical load of the tire, which can be expressed as

$$F_y = \mu_a \Phi F_z \tag{22}$$

where μ_a is the lateral friction coefficient of the tire, and Φ can be expressed as

$$\Phi = \begin{cases} 1 - e^{-10\left|\frac{V_{yi}}{|V_{xi}| + 0.01}\right|} & V_{yi} > 0 \\ e^{-10\left|\frac{V_{yi}}{|V_{xi}| + 0.01}\right|} - 1 & V_{yi} \leq 0 \end{cases} \tag{23}$$

where V_{xi} and V_{yi} are the longitudinal sub-velocities and lateral sub-velocities of each tire. According to the above equation, the direction of tire lateral force changes with the direction of the tire lateral sub-velocities.

(4) Rolling resistance torque

During the rolling process of the wheel, the tire will also be affected by the rolling resistance torque, which can be expressed as

$$M_y = \mu_r R_0 F_z \tag{24}$$

where μ_r is the coefficient of rolling resistance torque.

The longitudinal resistance torque of the wheel can be written as

$$M_R = R_0 F_x + M_y \tag{25}$$

When the helicopter brakes, the braking torque M_b is superimposed with the longitudinal resistance torque of the wheel. Under the action of the two torques, the rotation speed of the helicopter wheel slows down.

1.4.5 Mechanics model of friction shimmy damper

In this paper, the helicopter tail landing gear is a strut landing gear, and the friction shimmy damper is installed between the outer cylinder and the inner cylinder[3], as shown in Fig.5.
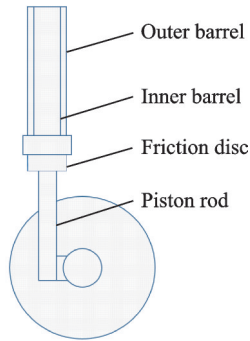
Fig.5   Schematic diagram of tail landing gear

The helicopter tail landing gear adopts dry friction shimmy damper, as shown in Fig.6, and the damping torque of friction can be expressed as

$$M_z = \frac{(D^3 - d^3)}{3(D^2 - d^2)} \mu F_{zn} \tag{26}$$

where D is the outer diameter of the friction shimmy damper; d the inner diameter of the friction shimmy damper; μ the friction coefficient of the friction shimmy damper; and F_{zn} the positive pressure of the friction shimmy damper.
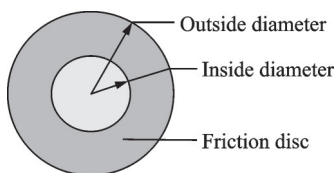
Fig.6   Schematic diagram of friction shimmy damper

The dynamic friction coefficient and the static friction coefficient are different. In general, the dynamic friction coefficient is smaller than the static friction coefficient. When using the dynamic friction coefficient μ_1, rotation resistance torque M_{z1} is obtained, and when the static friction coefficient μ_2 is taken, rotation resistance torque M_{z2} is obtained. The disc motion relationship is shown in Fig.7. Assuming that M_1 and M_2 are the rotational torques of the tire lateral force acting on the friction disc, they increase gradually from static state. When the rota-

tional torque M_1 of the tire lateral force at the friction disc is greater than the resistance torque M_{z2}, the friction disc starts to rotate and stops when the rotational torque M_1 is less than the dynamic friction torque M_{z1} at the friction disc. M_2 cannot rotate the friction disc. The red part in Fig.7 rotates, and the blue part does not rotate.
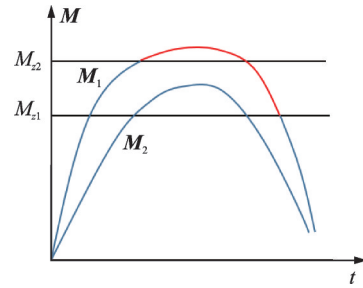
Fig.7   Rotation state of friction disc

2   Simulation Model

It is convenient to change the parameters of the model and simulate under different working conditions by using MATLAB to establish the helicopter model, which is convenient for researchers to achieve rapidly design.

According to the helicopter ground turning dynamic model in Section 1, the mechanical model of the buffer, the rotor tension model, the tire force model and the friction damper model are established in Matlab. After that, these subsystems are built into a whole helicopter model. Table 1 gives the parameters of helicopter model.

Table 1   Helicopter parameters

Parameter	Value
Mass / kg	12 000
Main wheel distance / mm	2 710
Tail wheel distance / mm	338
Distance between the center of gravity and the front tire / mm	1 370
Distance between center of gravity and tail wheel axle / mm	3 536
Main buffer structure stroke / mm	294.2
Tail buffer structure stroke / mm	256.9
Inner diameter of friction shimmy damper / mm	120
Outer diameter of friction shimmy damper / mm	140

Fig.8 shows the simulation model built according to the mathmatical model of buffer in Section 1.
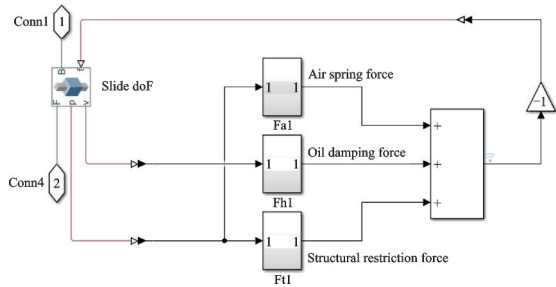
Fig.8   Mechanical model of landing gear buffer

Fig.9 is the simulation model of the tail landing gear friction disc of the pendulum reducer according to Section 1.4.5.
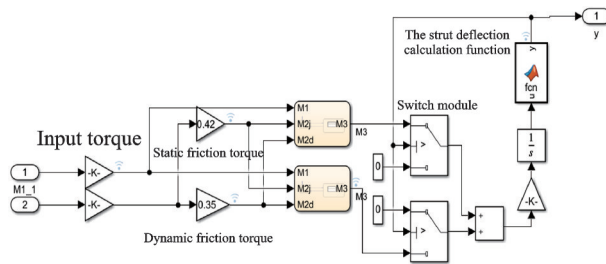
Fig.9   Mechanics model of friction shimmy damper

Fig.10 shows the tire force model established according to Section 1.4.4.
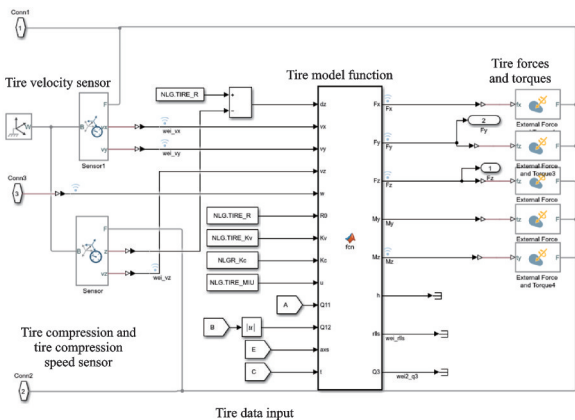
Fig.10   Tire mechanics model

The whole helicopter model is composed of above part models, as shown in Fig.11.

The thrust of helicopter ground taxiing is provided by the main rotor, the main rotor force forward inclination angle is θ, and the thrust can be changed by adjusting the inclination angle. Meanwhile, the thrust will also affect the helicopter landing gear's pressure on the ground, but the main rotor force remains unchanged in this process. Table 2
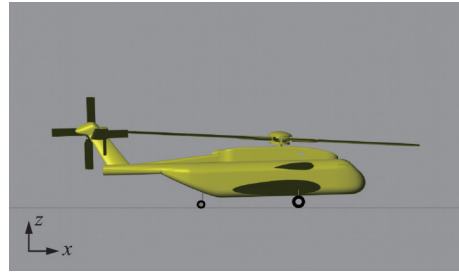
Fig.11   Helicopter model

gives the deflection angle to main rotor corresponding to taxiing speed.

Table 2   Deflection angle to main rotor corresponding to taxiing speed

Parameter	Value			
$\theta/(°)$	0.3	0.8	1.7	3.5
Taxing speed/$(m·s^{-1})$	0.5	1	2	4

3   Analysis of Simulation Results

3.1   Comparison of different tail rotor force

The taxiing speed v of helicopter is 2 m/s, and the critical tail rotor force is 3 055 N. Therefore, the tail rotor force F＝3 300, 3 500, and 3 700 N are selected for right angle turning simulation.

(1) The tail rotor force 3 300 N

At the 2 s of the simulation, the tail rotor force is linearly increased to 3 300 N to make the helicopter turn. Due to the large friction torque at the tail friction shimmy damper, the helicopter cannot return completely by the lateral force of the tail wheel. Therefore, when the fuselage turns 90° and the tail rotor force slowly stops, the reverse force of the tail rotor is applied to align the tail wheel until it stops.

As shown in Fig.12, the tail wheel begins to deflect at 3 s after the simulation starts, and stops deflecting at 6.3 s, maintaining at 13.8°, and the helicopter starts to make a steady turn. At 17 s, the fu-
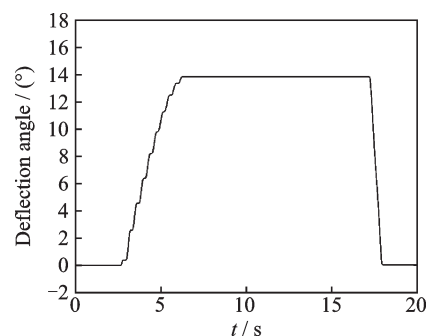
Fig.12   Tail wheel deflection angle (F＝3 300 N, v＝2 m/s)

selage has turned 90°, the tail rotor force gradually stops and increases in reverse, and the tail wheel starts to turn back at 17.2 s. At 17.9 s, the tail wheel deflection is 0°, the aligning is completed, and the helicopter begins to taxi straight.

As shown in Fig.13, the helicopter has a relatively small curvature during the initial turn, and the turning radius is about 19 m.
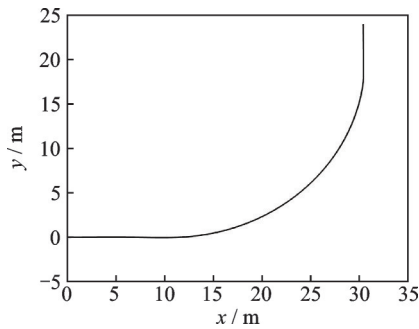
Fig.13   Projection curve center of gravity on the ground (F＝3 300 N, v＝2 m/s)

As shown in Fig.14, at the beginning of turning, the tail wheel lateral force is linearly related to the tail rotor force. When the tail rotor force reaches its maximum, the single tail wheel lateral force also reaches the peak value of 4 259 N. Then the helicopter starts to turn, and when the fuselage reaches 90°, the tail rotor force decreases first and then increases in reverse, making the tail wheel align.
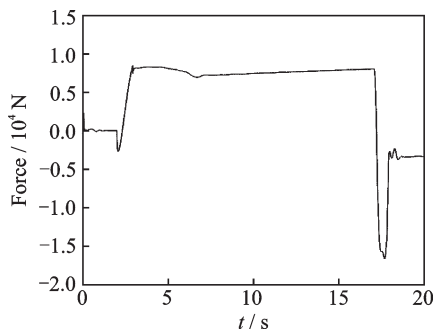
Fig.14   Tail wheel lateral force (F＝3 300 N, v＝2 m/s)

It can be seen from Fig.15 that the lateral force of the right main wheel rapidly increases to 583 N at 2 s during the right-angle turning. This is because when the reverse torque is applied, the reverse torque is mainly balanced by the friction between the tire and the ground in the condition of without the force of the tail rotor. With the increase of the tail rotor force, the lateral force of the right main
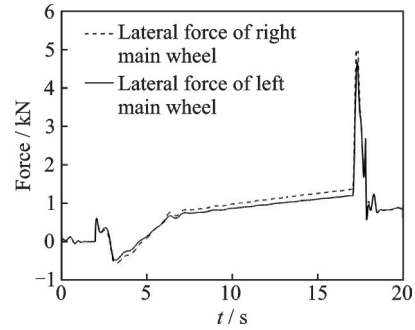
Fig.15   Main wheel lateral force (F＝3 300 N, v＝2 m/s)

wheel decreases and increases inversely, reaching the peak value of 559 N. After the tail wheel deflects, the lateral force increases slowly. When the fuselage reaches 90°, the tail rotor exerts a reverse force, and the lateral force of the main wheel increases rapidly, and decreases rapidly when the tail wheel returns to normal. Due to the existence of reverse torque, it cannot be reduced to zero and is stabilized at 809 N. Table 3 summarizes the above results.

Table 3   Simulation data corresponding to tail rotor force 3 300 N

Parameter	Value
Taxiing speed/(m·s^{-1})	2
Tail wheel deflection angle/(°)	13.8
Turning radius/m	19
Single tail lateral force (maximum)/N	4 259
Friction shimmy damper torque (maximum)/(N·m)	630
Lateral force of right main wheel (maximum)/N	559

(2) The tail rotor force 3 500 N

At 2 s of the simulation, the tail rotor force is linearly increased to 3 500 N to make the helicopter turn. The simulation data are shown in Table 4.

Table 4   Simulation data corresponding to tail rotor force 3 500 N

Parameter	Value
Taxiing speed/(m·s^{-1})	2
Tail wheel deflection angle/(°)	18.6
Turning radius/m	15
Single tail lateral force (maximum)/N	4 322
Friction shimmy damper torque (maximum)/(N·m)	621
Lateral force of right main wheel (maximum)/N	631

(3) The tail rotor force 3 700 N

At 2 s of the simulation, the tail rotor force is linearly increased to 3 700 N, which makes the helicopter turn. The simulation data are shown in Table 5.

Table 5 Simulation data corresponding to tail rotor force 3 700 N

Parameter	Value
Taxiing speed/(m·s^{-1})	2
Tail wheel deflection angle/(°)	23.4
Turning radius/m	13
Single tail lateral force (maximum)/N	4 517
Friction shimmy damper torque (maximum)/(N·m)	650.5
Lateral force of right main wheel (maximum)/N	707

According to the above three working conditions of Tables 3, 4 and 5, it can be concluded that the greater the tail rotor force, the greater the tail wheel angle, the greater the lateral force at the main wheel and the tail wheel as the tail rotor force increase. The increase of tail rotor force has a significant impact on the rotation angle of the tail wheel.

3.2 Comparison of different turning speeds

In this set of simulations, right-angle turning of the helicopter is simulated with three groups of taxiing speeds of 1, 2, 4 m/s. The tail rotor force is 3 300 N, and the tail wheel stability distance is 72 mm.

(1) Taxiing speed 1 m/s

At 2 s of the simulation, the tail rotor force is linearly increased to 3 300 N to make the helicopter turn.

As shown in Fig.16, the tail wheel begins to deflect at 2.8 s after the beginning of the simulation,
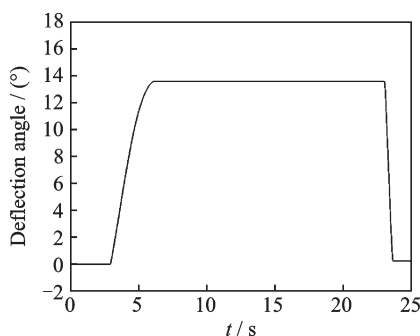
Fig.16 Tail wheel deflection angle (F＝3 300 N, v＝1 m/s)

and stops deflecting at 6.4 s, maintaining at 13.57°, and the helicopter begins to make a steady turn. At 23 s, the fuselage has turned 90°, the tail rotor force gradually stops and increases in reverse, and the tail wheel begins to align at 23.2 s. At 24 s, the tail wheel deflection angel is 0°, the aligning is completed, and the helicopter starts to taxi in a straight line.

As shown in Fig.17, the trajectory of the center of gravity is close to a quarter circle on the ground, and the turning radius is 20 m.
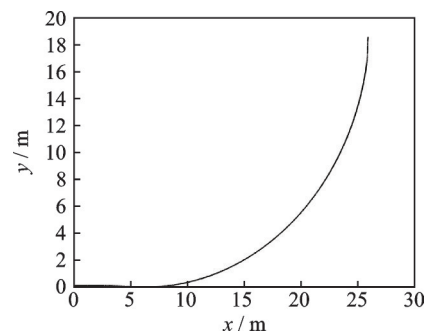
Fig.17 Projection curve of center of gravity on the ground (F＝3 300 N, v＝1 m/s)

As shown in Fig.18, at the beginning of the turn, the tail wheel lateral force is linearly related to the tail rotor force. When the tail rotor force reaches the maximum, the lateral force of the single tail wheel also reaches the peak value of 4 271 N. When the fuselage reaches 90°, the lateral force of the single tail wheel first decreases and then increases in reverse, making the tail wheel align.
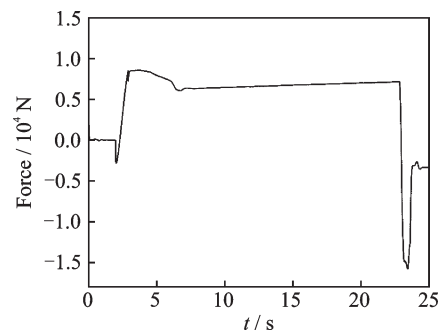
Fig.18 Tail wheel lateral force (F＝3 300 N, v＝1 m/s)

In the process of right-angle turning, the lateral force of the right main wheel rapidly increases to 636 N within 2 s, as shown in Fig.19. As the tail rotor force increases, it first decreases and then increases in reverse, reaching the peak value of 700 N. After that, due to the sudden change of the tail

rotor force, the lateral force of the right main wheel is stabilized at 849 N when the process of tail wheel aligning is finished. The simulation data corresponding to taxiing speed of 1 m/s are given in Table 6.
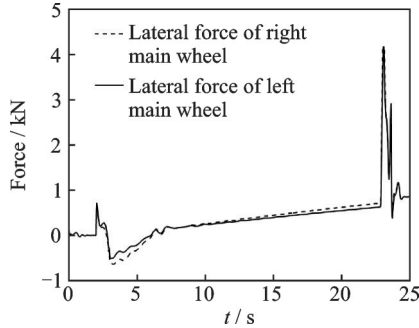
Fig.19   Tail wheel lateral force ($F=3\,300$ N, $v=1$ m/s)

Table 6   Simulation data corresponding to taxiing speed of 1 m/s

Parameter	Value
Taxiing speed/(m·s⁻¹)	1
Tail wheel deflection angle/(°)	13.6
Turning radius/m	20
Single tail lateral force (maximum)/N	4 271
Friction shimmy damper torque (maximum)/(N·m)	630
Lateral force of right main wheel (maximum)/N	559

(2) Taxiing speed 4 m/s

In this simulation, the taxiing speed is set to 4 m/s, and the tail rotor force was linearly increased to 3 300 N at 2 s of the simulation to make the helicopter turn. The simulation data corresponding to taxxing speed of 4 m/s are given in Table 7.

Table 7   Simulation data corresponding to taxiing speed of 4 m/s

Parameter	Value
Taxiing speed/(m·s⁻¹)	4
Tail rotor force/N	3 300
Tail wheel deflection angle/(°)	18.8
Turning radius/m	14
Single tail lateral force (maximum)/N	4 250

The simulation data of taxiing speed of 2 m/s is shown in Table 3. It can be concluded from Tables 3, 6, and 7 that when the tail rotor force is the same, the greater the taxing speed, the easier it is to turn. The influence of taxing speed on the lateral force of tail wheel is not obvious.

3.3   Stationary turn

For the helicopter in a completely static state, it is impossible to calculate the lateral force and frictional resistance of the tire by the relationship of the wheel deflection angle, therefore, an empirical formula for calculating the friction force of the stationary tire is referred to. The turning of the landing gear is subject to the uniformly distributed friction force of the ground against the tires. The uniformly distributed friction force produces two frictional resistance torques: The uniformly distributed friction torque and the torque generated by the equivalent concentrated friction force to the piston rod, which can be expressed as

$$M_{j} = 0.8P_{VN}\left\{\frac{3a}{4\pi}\right\} \tag{27}$$

$$M_{T} = M_{j} + 0.8bP_{VN} \tag{28}$$

$$a = 0.85d'\sqrt{(\delta/d') - (\delta/d')^2} \tag{29}$$

where M_{j} is the uniformly distributed friction torque, P_{VN} the vertical load of the landing gear strut, a the half length of the tire touching the ground, b the stability distance, and d' the wheel diameter.

In the static state, the helicopter completely relies on the tail rotor force to make the tail wheel rotate around the axis of the strut. Initially, the tail rotor force is linearly increased to 4 655 N, meanwhile, the tail wheel begins to rotate under the action of driving force. Through the simulation, it is found that this kind of turning is unstable. After the helicopter moves, it is switched to the dynamic simulation model, the criterion for switching is that when the tail wheel starts to deflect a small angle, the tail wheel slips slightly, which means a smooth transition to the dynamic simulation model. And the tail rotor force is set to 4 357 N after switching.

It can be concluded from Fig.20 that the trajectory of each point can be obviously divided into two sections. In the first section, the static turning theory is applied, and the tail wheel is completely taxiing on the ground. The second section is switched to the dynamic turning state, and the helicopter turns on the ground with a turning radius of 7 m.

As shown in Fig.21, the tail wheel angle in-
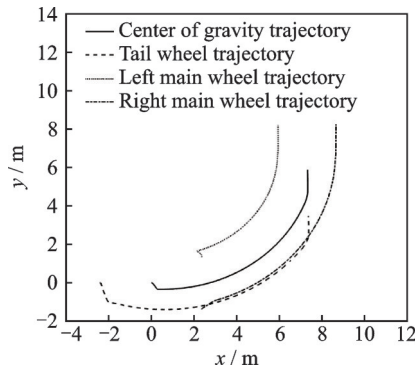
Fig.20   Projection of each point of fuselage on the ground

creases linearly when the tail rotor force is applied within 1 s to 2 s, and the rotation angle increases to 18°, and remains unchanged after removing the tail rotor force from 2 s to 2.5 s. At 2.8 s, the torque transferred from the tail wheel to the tail friction plate is greater than the static friction torque of the tail wheel, and the tail wheel begins to deflect. At 4.2 s, the tail wheel stops deflecting and the tail wheel deflection angle remains at 28°. When the simulation runs to 11 s, the tail wheel starts to align, and the process is completed at 11.8 s, then it enters the straight-line taxiing state.
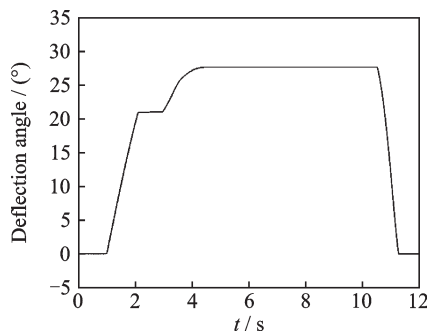
Fig.21   Tail wheel deflection angle

As shown in Fig.22, when switching to the dynamic turning model, there is a sudden change in the lateral force at 2.5 s. Later, with the increase of the tail rotor force, the lateral force gradually in-
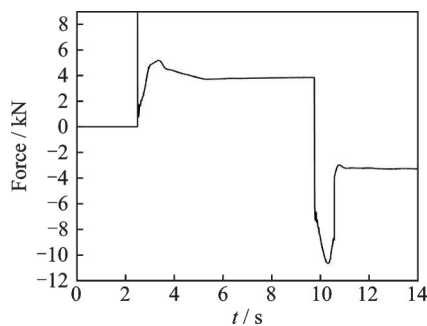
Fig.22   Lateral force of tail wheel

creases and finally reaches the maximum value of 5 115 N, and the lateral force reaches 3 815 N after the steady-state turning.

As shown in Fig.23, when switching to the dynamic model, there is a sudden change in the lateral force of the main wheel, too. In the process of right-angle turning, the lateral force of the right main wheel first increases with the increase of the tail rotor force, finally reaching the peak value of 2 962 N. Then the helicopter begins to turn. When the tail rotor exerts the force in reverse to make the tail wheel align, the lateral force of the right main wheel rapidly reduced to zero. The data of ground static right-angle turning are given in Table 8.
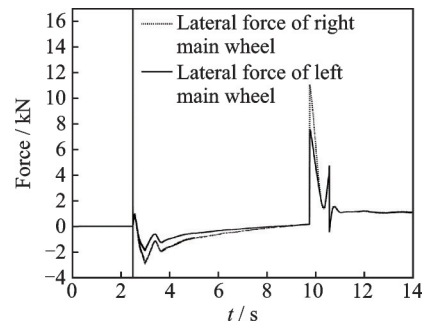
Fig.23   Lateral force of main wheel

Table 8   Data of ground static right-angle turning

Parameter	Value
Taxiing speed/(m·s^{-1})	0
Tail rotor force (After the tail wheel rotates)/N	4 655
Tail wheel deflection angle/(°)	28
Turning radius/m	7
Single tail lateral force (maximum)/N	5 115
Tail deflection angle (maximum)/(°)	3.2
Lateral force of right main wheel (maximum)/N	2 962

3. 4   Comparison of different tail wheel stability distance

In this set of simulations, the tail wheel stability distance is doubled to 144 mm, and after obtaining the critical tail rotor force, the three groups of tail rotor force are set to 2 300, 2 500, and 2 700 N, respectively.

(1) Tail rotor force 2 300 N

At 2 s of the simulation, the tail rotor force is linearly increased to 2 300 N to make the helicopter turn. The simulation data corresponding to tail rotor force 2 300 N are given in Table 9.

Table 9   Simulation data corresponding to tail rotor force 2 300 N

Parameter	Value
Taxiing speed/(m·s⁻¹)	2
Tail rotor force/N	2 300
Tail wheel deflection angle/(°)	12.6
Turning radius / m	21
Single tail lateral force (maximum)/N	2 133
Friction shimmy damper torque (maximum)/(N·m)	616
Lateral force of right main wheel (maximum)/N	643

(2) Tail rotor force 2 500 N

At 2 s of the simulation, the tail rotor force is linearly increased to 2 500 N to make the helicopter turn. The simulation data corresponding to tail rotor force 2 500 N are given in Table 10.

Table 10   Simulation data corresponding to tail rotor force 2 500 N

Parameter	Value
Taxiing speed/(m·s⁻¹)	2
Tail rotor force/N	2 500
Tail wheel deflection angle/(°)	17.9
Turning radius/m	16
Single tail lateral force (maximum)/N	2 265
Friction shimmy damper torque (maximum)/(N·m)	652
Lateral force of right main wheel (maximum)/N	643

(3) Tail rotor force 2 700 N

At the 2 s of the simulation, the tail rotor force is linearly increased to 2700 N to make the helicopter turn. The simulation data corresponding to tail rotor force 2 700 N are given in Table 11.

Table 11   Simulation data corresponding to tail rotor force 2 700 N

Parameter	Value
Taxiing speed/(m·s⁻¹)	2
Tail rotor force/N	2 700
Tail wheel deflection angle/(°)	23.1
Turning radius/m	14
Single tail lateral force (maximum)/N	2 260
Friction shimmy damper torque (maximum)/(N·m)	691
Lateral force of right main wheel (maximum)/N	633

Comparing Tables 3, 4, 5 with Tables 9, 10, 11, it can be concluded that the stability distance has a decisive effect on the tail wheel deflection an-

gle. When the tail wheel stability distance is doubled, the tail rotor force required for the same angle of the tail wheel is reduced by one-third, and the lateral force of the tail wheel is reduced by half.

4   Conclusions

(1) The six-degree-of-freedom dynamic model of helicopter taxiing and turning is established, including the airframe dynamics model, the mathematical model of related forces and the tire mechanics model.

(2) The influence of speed and tail rotor force on helicopter turning radius is analyzed. When the taxing speed is the same, the angle of the tail wheel increases with the increase of the force of the tail rotor. When the tail rotor force is the same, the tail wheel angle increases with the increase of taxing speed.

(3) It is analyzed that in the static state, the helicopter only uses the tail rotor force to make a turn on the ground, and it needs to provide bigger tail rotor force to turn the tail wheel than other states by nearly 50%. It is concluded that it is difficult to turn in the static state.

(4) The influence of different tail wheel stability distance on helicopter turning is discussed, and it is concluded that the stability distance has a significant effect on tail wheel deflection. When the stable distance of the tail wheel is doubled, the tail rotor tension required for the tail wheel to rotate at the same angle is reduced by about 30%, and the lateral force of the tail wheel is reduced by nearly 50%.

References

[1] YANG Yongwen, MENG Qingsong, LYU Changshaeng. Research on helicopter ground motion dynamics[C]//Proceedings of the 24th National Helicopter Annual Meeting. Nanjing: Chinese Society of Aeronautics and Astronautics, 2008.(in Chinese)

[2] CHEN Zhifu. Advanced helicopter landing gear dynamic investigation[D]. Nanjing: Nanjing University of Aeronautics and Astronautics, 2009. (in Chinese)

[3] SUN Weimin, ZHANG Mei. Damping characteristics analysis of a helicopter friction damper[J]. Helicopter Technique, 2018(2): 25-28,33. (in Chinese)

[4] XU Qinyong, YIN Shihui, XU Yumao. Fight dynamics analysis of helicopter taxiing[J]. Helicopter Tech-

nique，2015(2)：6-10. (in Chinese)

[5] LI Yongping. Design of a new type of composite shock absorber and study on its crashworthiness [D]. Nanjing：Nanjing University of Aeronautics and Astronautics，2018. (in Chinese)

[6] YANG Lifang. The simulation analysis on the tire stiffness and tail-wheel shimmy of an aircraft[D]. Nanjing：Nanjing University of Aeronautics and Astronautics，2012. (in Chinese)

[7] YANG Guoping. Aircraft tire model and research of simulation of aircraft tire movement on the ground [D]. Nanjing：Civil Aviation Fight University of China，2009. (in Chinese)

[8] LI Youyi, LI Songwei, XU Kun, et al. Dynamics modeling and simulation of helicopter landing gear [C]//Proceedings of the 2012 Chinese Guidance, Navigation and Control Conference. Beijing, China：[s.n.], 2012. (in Chinese)

[9] DONG Mingming. Design and dynamic analysis of a helicopter landing gear parameters[D]. Nanjing：Nanjing University of Aeronautics and Astronautics，2010. (in Chinese)

[10] SIVAPRAKASAM S. Helicopter landing gear vibration analysis using Lagrange method [J]. Vibroengineering Procedia，2018. DOI：10.21595/vp. 2018. 20363.

[11] PRITCHARD J. An overview of landing gear dynamics：NASA TM-1999-209143 [R]. [S. l.] ：NASA，1999.

[12] YU Zhi，SHEN Gongzhang，YANG Chao. Helicopter flight dynamics simulation model based on Simulink [J]. Journal of System Simulation，2006，18(10)：2730-2733. (in Chinese)

[13] ZHANG Ming. Research on some key technologies of aircraft ground dynamics [D]. Nanjing：Nanjing University of Aeronautics and Astronautics，2009. (in Chinese)

[14] HU G C，WU J，LIU X Y，et al. Dynamic behaviors of helicopter rotor in vertical landing [J]. Acta Aeronautica et Astronautica Sinica，2018，39(6)：96-105. (in Chinese)

[15] PARK Wansoo，Hwang Jaeup，Hyun Youngho，Hwang Jaehyuk，Bae Jaeseoung，Kim Taewook. Dynamic characteristics analysis of landing gear that consider 6-degree of freedom of helicopter[J]. Journal of Aerospace System Engineering，2008，2(1)：1-6.

Authors   Dr. **LI Jin** received the M.S degree in aircraft design from Nanjing University of Aeronautics and Astronautics (NUAA), China, in 2007. In May 2007, he joined the China Helicopter Research and Development Institute, Jingdezhen, China. His research interests include helicopter design and structure design.

Prof. **ZHANG Ming** received the Ph.D. degree in aircraft design from Nanjing University of Aeronautics and Astronautics, China, in 2009. In June 2009, he joined the Key Laboratory of Fundamental Science for National Defense-Advanced Design Technology of Flight Vehicle, College of Aerospace Engineering, NUAA, Nanjing, China. His research interests include aircraft design, dynamics and landing gear system.

Author contributions   Dr. **LI Jin** designed the study, analyzed the study and wrote the manuscript. Prof. **ZHANG Ming** designed the method, implemented the model and revised the manuscript. Dr. **HUANG Jianxin** analyzed the result. Dr. **CHEN Xiang** contributed to the discussion and background of the study. Dr. **WEI Xiyang** contributed to the dynamics simulation. All the authors commented on the manuscript draft and approved the submission.

Competing interests   The authors declare no competing interests.

（Production Editor：SUN Jing）

直升机地面转弯运动特性研究

李　进[1,2]，张　明[2]，黄建新[1]，陈　翔[1]，卫夕阳[2]

（1.中国直升机设计研究所,景德镇 333001,中国；
2.南京航空航天大学飞行器先进设计技术国防重点学科实验室,南京 210016,中国）

摘要：直升机地面转弯通过尾桨拉力和地面对尾轮的摩擦力实现,当直升机重心靠后时出现低速滑行或静止状态下转弯困难的现象。本文以某型号直升机为研究对象,基于动力学基础理论建立了直升机地面转弯运动动力学模型。该模型考虑直升机机体六自由度运动模型、起落架缓冲器运动模型、轮胎力学模型和支柱摩擦盘摩擦特性,对直升机地面直角转弯及静态转弯进行动力学仿真,并分析尾桨拉力、滑行速度、尾轮稳定距等参数对转弯动态响应的影响规律。结果表明,通过增大尾轮稳定距可提高直升机地面转弯性能。

关键词：直升机地面运动;动力学分析;被动转弯;起落架